Tetrahedral Element Shape Optimization via the Jacobian Determinant and Condition Number

Lori A. Freitag
Mathematics and Computer Science Division
Argonne National Laboratory
Argonne, IL 60439
freitag@mcs.anl.gov

Patrick M. Knupp
Parallel Computing Sciences Department
Sandia National Laboratories
M/S 0441, P.O. Box 5800
Albuquerque, NM 87185-0441
pknupp@sandia.gov

Abstract. We present a new shape measure for tetrahedral elements that is optimal in the sense that it gives the distance of a tetrahedron from the set of inverted elements. This measure is constructed from the condition number of the linear transformation between a unit equilateral tetrahedron and any tetrahedron with positive volume. We use this shape measure to formulate two optimization objective functions that are differentiated by their goal: the first seeks to improve the average quality of the tetrahedral mesh; the second aims to improve the worst-quality element in the mesh. Because the element condition number is not defined for tetrahedra with negative volume, these objective functions can be used only when the initial mesh is valid. Therefore, we formulate a third objective function using the determinant of the element Jacobian that is suitable for mesh untangling. We review the optimization techniques used with each objective function and present experimental results that demonstrate the effectiveness of the mesh improvement and untangling methods. We show that a combined optimization approach that uses both condition number objective functions obtains the best-quality meshes.

Keywords. Mesh Improvement, Optimization-based Mesh Smoothing, Mesh Quality, Mesh Untangling

1 Introduction

Local mesh smoothing algorithms are commonly used for simplicial mesh improvement. These methods relocate a set of adjustable vertices, one at a time, to improve mesh quality in a neighborhood of that vertex. The new grid point position is determined by considering a local submesh containing the adjustable, or *free vertex*, v, and its incident vertices and elements. For example, in Figure 1, we show a two-dimensional local submesh with three possible locations for v. The leftmost local submesh shows a valid but poor-quality mesh, the middle submesh shows a higher-quality valid mesh, and the rightmost shows an invalid mesh with inverted elements. Overall improvement in the mesh is obtained by performing some number of sweeps over the set of adjustable vertices.
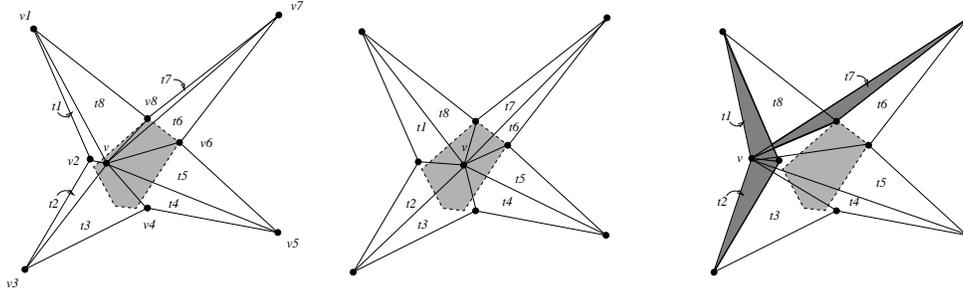
Figure 1: A local submesh with three possible locations for v.

The most commonly used local mesh smoothing technique is Laplacian smoothing [6, 16] which moves the free vertex to the geometric center of its incident vertices. Laplacian smoothing is computationally inexpensive but does not guarantee improvement in the element quality.

To address this problem, several optimization-based approaches to mesh smoothing have been developed in recent years, for example, [19, 11, 1, 18, 13]. In these techniques, the local submesh is evaluated according to some objective function based on a quality metric, q_i, such as element angle or aspect ratio. Function and, possibly, gradient information are used to relocate the free vertex in such a way that the objective function is optimized. For example, if the quality metric under consideration is element angle, the leftmost submesh in Figure 1 shows an initial position for v that results in three poor-quality elements, $t1$, $t2$, and $t7$. The middle submesh in Figure 1 shows the position of v that optimizes the element angle. We note that if the initial mesh contains inverted elements, objective functions that work well for mesh quality improvement may not be appropriate for mesh untangling [10].

Several optimization objective functions based on geometric criteria have been proposed for *a priori* improvement of a simplicial mesh. For example, Bank proposed a ratio of triangle area to edge length squared for two-dimensional meshes [2], Shephard and Georges proposed a similar ratio of volume to face areas for tetrahedral meshes [19], Freitag et al. used angle-based measures for both two- and three-dimensional meshes [9, 11], and Knupp has proposed a number of shape quality measures derived from simplicial element Jacobian matrices [13, 14]. Canann et al. proposed a distortion metric for both triangles and quadrilaterals that could be used with both valid and inverted elements [18]. In addition, *a posteriori*

metrics have been proposed to improve finite element meshes by optimizing solution error indicators [1].

In Section 2, we propose a new quality metric for the *a priori* improvement of tetrahedral meshes. The metric is based on the condition number of the linear transformation from an equilateral tetrahedron to any arbitrary tetrahedron. We show that the condition number metric is a tetrahedral shape measure according to the formal definition given in [4] and that it is optimal in that it gives the distance of a tetrahedron to the set of inverted elements. Our purpose in introducing this previously overlooked metric is to show that it is effective and well-motivated. From a theoretical perspective the metric is not ad-hoc and is notable in that it is not derived from geometric quantities such as edge lengths, angles, and volumes. We have not proved, but suspect that, the metric is equivalent (in the sense of Liu and Joe [15]) to a number of other well-known tetrahedral shape measures. From a practical perspective, we only claim that the metric is no more expensive to compute than most other shape measures and that it is an effective means of improving global mesh quality.

In Section 3, we formulate two optimization objective functions using the element condition number that are suitable for mesh improvement if the initial mesh is valid. The first objective function targets the improvement of average element quality; the second targets the improvement of the worst element quality. If the initial mesh is not valid, this shape measure cannot be used for mesh improvement as it is not defined for inverted elements. In this case we use an objective function based on the determinant of the Jacobian that is suitable for untangling the inverted elements. In previous papers, we have independently proposed optimization techniques for mesh untangling [10], mesh improvement as measured by average element quality [13], and mesh improvement

as measured by extremal element quality [11], and we review these optimization techniques in Section 3.2.

In Section 4, we present numerical results for each of the mesh improvement strategies using the condition number shape measure on four tetrahedral meshes. We compare each technique to a baseline Laplacian smoother, and illustrate that in each test case, a combined optimization approach produces the best-quality meshes. We also show that the techniques can achieve high-quality meshes even when starting with an invalid mesh, by combining the mesh improvement strategies with the mesh untangling approach. Finally, in Section 5, we offer concluding remarks and directions for future research.

2 Tetrahedral Jacobian Matrices and Condition Numbers

In this section we discuss the linear transformations associated with tetrahedral elements. Figure 2 illustrates the situation in two dimensions. The matrix A (referred to as the Jacobian matrix) transforms points in the reference triangle (a right-angled triangle) to points in an arbitrary physical triangle. The matrix W transforms the reference triangle to an equilateral triangle. The matrix $S = AW^{-1}$, which transforms the ideal triangle to the physical triangle, is critical because it measures the deviation of the physical triangle from the ideal shape. A new tetrahedral shape measure based on S is constructed using matrix norms and the condition number.
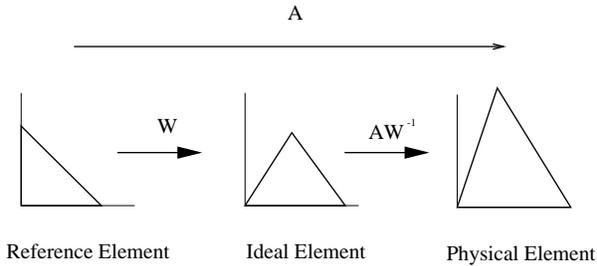

Figure 2: The relationship between the linear transformations and the reference, ideal, and physical elements

2.1 Tetrahedral Jacobian Matrices

Let T be an arbitrary tetrahedral element consisting of four vertices v_n, $n = 0, 1, 2, 3$ with coordinates $\mathbf{x}_n \in R^3$. Let $\mathcal{V}(T)$ denote the volume of the tetrahedron. Define edge vectors $e_{k,n} = \mathbf{x}_k - \mathbf{x}_n$ with $k \neq n$ and $k = 0, 1, 2, 3$ (note that $e_{n,k} = -e_{k,n}$). Vertex v_n has three attached edge vectors, $e_{n+1,n}$, $e_{n+2,n}$, and $e_{n+3,n}$, where the indices are taken modulo four. Define the Jacobian matrix at node n (denoted by A_n) to consist of the columns of the triplet of attached edge vectors, namely,

$$A_n = (-1)^n \left(\begin{array}{ccc} e_{n+1,n} & e_{n+2,n} & e_{n+3,n} \end{array} \right).$$

Let α_n be the determinant of A_n. A right-handed rule is assumed for the edge-ordering so that elements with positive volume correspond to $\alpha_n > 0$.

Theorem 1. The determinants $\alpha_n = \alpha_0$ for $n = 1, 2, 3$.
Proof.
Let M be the following constant matrix

$$M = \left(\begin{array}{ccc} 1 & 1 & 1 \\ -1 & 0 & 0 \\ 0 & -1 & 0 \end{array} \right).$$

The determinant of M equals 1. A direct calculation shows that

$$A_n = A_0 \, M^n$$

for $n = 1, 2, 3$. Taking the determinant of this expression gives $\alpha_n = \alpha_0$. §

It is well known that the volume of a tetrahedron is one-sixth of the Jacobian determinant [12], hence $\alpha_0 = 6\,\mathcal{V}(T)$ and $\mathcal{V}(T) > 0$ if and only if $\alpha_0 > 0$. An element is said to be *invertible* if and only if $\alpha_0 > 0$.

Matrix norms are a critical part of the theory to be presented. Let I be the identity matrix and S be an arbitrary matrix. The Frobenius norm of S is defined in terms of the trace:

$$\mid S \mid = [\, tr(S^T S)\,]^{1/2}.$$

The Frobenius norm is invariant to rotation matrices, that is, $\mid SR \mid = \mid RS \mid = \mid S \mid$, where R is a rotation matrix ($R^T R = I$, $\mid det(R) \mid = 1$). If S is invertible, then S^{-1} exists, and one can define the adjoint matrix of S:

$$adj\,(S) = \sigma\, S^{-1},$$

where $\sigma = det(S)$.

One can easily show that the following relationships hold for the Jacobian matrix:

$$
\begin{aligned}
\mid A_n \mid^2 \ = \ & \mid e_{n+1,n} \mid^2 + \mid e_{n+2,n} \mid^2 + \\
& \mid e_{n+3,n} \mid^2, \ \text{and} \\
\mid adj\,(A_n) \mid^2 \ = \ & \mid e_{n+1,n} \times e_{n+2,n} \mid^2 + \\
& \mid e_{n+2,n} \times e_{n+3,n} \mid^2 + \\
& \mid e_{n+3,n} \times e_{n+1,n} \mid^2 .
\end{aligned}
$$

These provide a geometric interpretation of the norms. The norm-squared of A_n is the sum of the lengths-squared of the attached edge vectors and the norm-squared of the adjoint is the sum of the squares of the areas of the attached triangular faces.

Unlike the determinant α_n, the norms of A_n and $adj\,(A_n)$ are not independent of n because not all of the lengths and areas of the tetrahedron affect the result for A_n. This situation can be remedied, as will be shown next.

Define an equilateral tetrahedron T_e to have sides of length one and four vertices with the coordinates $(0,0,0)$, $(1,0,0)$, $(1/2,\sqrt{3}/2,0)$, and $(1/2,\sqrt{3}/6,\sqrt{2}/\sqrt{3})$. This tetrahedron serves as the ideal element. Let W_n be the Jacobian matrix at the nth vertex of T_e. For example,

$$
W_0 = \begin{pmatrix} 1 & 1/2 & 1/2 \\ 0 & \sqrt{3}/2 & \sqrt{3}/6 \\ 0 & 0 & \sqrt{2}/\sqrt{3} \end{pmatrix}
$$

and $w_0 = det(W_0) = \sqrt{2}/2$.

Theorem 2.
Let T be any tetrahedron, with Jacobian matrices A_n. Let S_n be the linear transformation that takes W_n to A_n. Then $S_n = A_0\,W_0^{-1}$, that is, S_n is independent of n.
Proof.
By definition, $S_n W_n = A_n$. If $n = 0$, $S_0 = A_0\,W_0^{-1}$. Theorem 1 applies to the matrices W_n of T_e. Thus $W_n = W_0\,M^n$ for $n = 1,2,3$. Since $A_n = A_0\,M^n$, we have the stated result. §
In other words, there exists a unique linear transformation between the logical tetrahedron T_e and the physical tetrahedron T. Because of this result, let us denote W_0 by W and w_0 by w.

Theorem 3.
$\mid A_n W^{-1} \mid = \mid A_0 W^{-1} \mid$ and $\mid W A_n^{-1} \mid = \mid W A_0^{-1} \mid$.
Proof.
The result for $n = 0$ is immediate. Define the matrix

$R = WMW^{-1}$, where M is defined in the proof of Theorem 1. A direct calculation shows that R is a rotation matrix with a positive determinant. Therefore, $det(R^n) = 1$ and $(R^n)^T R^n = I$ for $n = 1,2,3$; that is, R^n is a rotation matrix. Hence

$$
\begin{aligned}
\mid A_n W^{-1} \mid \ &= \ \mid A_0 M^n W^{-1} \mid \\
&= \ \mid A_0 W^{-1} R^n \mid \\
&= \ \mid A_0 W^{-1} \mid .
\end{aligned}
$$

Similarly, the second result can be proved by observing that $W A_n^{-1} = (A_n W^{-1})^{-1} = (R^n)^{-1} W A_0^{-1}$ and showing that $(R^n)^{-1}$ is a rotation matrix. §
This theorem shows that the norms $\mid A_n W^{-1} \mid$ and $\mid W A_n^{-1} \mid$ are independent of n.

2.2 Tetrahedral Condition Numbers

Let T_+ be any tetrahedron with positive volume. Then A_n^{-1} exists, and one can compute the weighted *condition number* of the matrix A_n

$$
\kappa_w(A_n) = \mid A_n W^{-1} \mid \mid (A_n W^{-1})^{-1} \mid .
$$

Since $(A_n W^{-1})^{-1} = W A_n^{-1}$, Theorem 3 shows that $\kappa_w(A_n)$ is independent of n. This is not true for the unweighted condition number $\kappa(A_n) = \mid A_n \mid \mid A_n^{-1} \mid$. Now let A be any of the four Jacobian matrices of an invertible tetrahedron. Let $\kappa_w(A) = \mid AW^{-1} \mid \mid WA^{-1} \mid$. Recall that S is the linear transformation taking T_e to T_+; hence $\kappa_w(A) = \mid S \mid \mid S^{-1} \mid = \kappa(S)$. That is, $\kappa(S)$ *measures the condition number of the linear transformation between the logical and physical tetrahedra.*

Theorem 4.
Let S be derived from a tetrahedron with positive volume. Then $3/\kappa(S)$ is a tetrahedral shape measure.
Proof.
We use the formal definition given in [4] to prove this assertion.

First, it is clear that $\mid S \mid$ is a continuous function of the coordinates of T_+, and likewise so is $\mid S^{-1} \mid$. Therefore $\kappa(S)$ is a continuous function of the coordinates of any tetrahedron with positive volume.

Second, the Jacobian matrix is invariant to translations so $\kappa(S)$ is invariant to translations. Let $\tilde{A} = \lambda R A$ with $\lambda > 0$ and R be a rotation matrix corresponding to a uniform scaling and rotation

of the tetrahedron. Let $\tilde{S} = \tilde{A}W^{-1}$. Since the Frobenius norm is invariant under rotations, it is clear that $\kappa(\tilde{S}) = \kappa(S)$. Finally, $\kappa(S)$ is invariant to scaling since for any $\epsilon \in R$, the definition of condition number directly shows that $\kappa(\epsilon S) = \kappa(S)$.

Third, it is clear that $0 < 3/\kappa(S)$. For any matrix, $\mid S \mid^2$ is the sum of the squares of its singular values σ_i. Thus

$$\kappa^2(S) = \sum_{i,j} (\sigma_i/\sigma_j)^2.$$

This is a continuous function of three variables and its minimum may be found by computing the solution to $\partial \kappa^2/\partial \sigma_i = 0$ with $i = 1, 2, 3$. The solution is $\sigma_i = \sigma$ where σ is any positive constant. Hence $\kappa \geq 3$. This shows that $0 < 3/\kappa \leq 1$, as required for a tetrahedral shape measure.

Fourth, suppose $3/\kappa = 1$. Then the singular values of S must be constant and $S = \sigma R$. Then the Jacobian matrix associated with the tetrahedron must have the form $A = \sigma R W$, in other words, $3/\kappa$ attains its maximum value only if the tetrahedral element is a rotation and uniform scaling of the logical tetrahedron. The converse is easy to show.

Fifth, the definition of a degenerate tetrahedral element given in [4] is somewhat vague. As noted, a tetrahedron with a small volume is not necessarily degenerate. This is reflected in the properties of the condition number. For example, if $A = \epsilon W$, where $0 < \epsilon << 1$, then $\alpha = \epsilon^3 \, det(W)$ is small, but $3/\kappa_w(\epsilon W) = 1$. Thus a tetrahedron with small volume does not necessarily make $3/\kappa(S)$ large. Reference [4] gives an example of a degenerate tetrahedron, one whose volume goes to zero but at least some of the lengths do not. Suppose there exist constants b and c such that $0 < b \leq \mid S \mid$ and $0 < c \leq \mid adj(S) \mid$. Then both $\mid A \mid$ and $\mid adj(A) \mid$ are bounded below by a positive constant. Since

$$\kappa(S) = \mid S \mid \mid adj(S) \mid /\sigma,$$

the limit of $3/\kappa(S)$ as $\alpha \to 0$ is zero. Hence, the condition number satisfies the requirement that a shape measure go to zero for a degenerate element, at least for the given example. The second author reported numerical experiments in [14] like those described in [17] which show that the common tetrahedral shape degeneracies can be detected by the condition number. In fact, the condition number provides a rigorous definition of a degenerate element. Let $0 < \epsilon << 1$ be given. Then T_+ is degenerate if $3/\kappa(S) < \epsilon$. §

It is possible to show that at least some of the other weighted nondimensional objective functions given in [14] are also tetrahedral shape measures. The distinguishing feature between the condition number and these other measures is given in the following well-known theorem [3] adapted to our current setting.

Theorem 5.
$1/\kappa(S)$ is the greatest lower bound for the distance of S to the set of singular matrices.
Proof.
Let S and X be 3×3 matrices with S non-singular and $S + X$ singular. Write $S + X = S(I + S^{-1}X)$. If $\mid S^{-1}X \mid < 1$, then $I + S^{-1}X$ is nonsingular. This would mean that $S + X$ is nonsingular, so we must have $\mid S^{-1}X \mid \geq 1$. But $1 \leq \mid S^{-1}X \mid \leq \mid S^{-1} \mid \mid X \mid$; hence $\mid X \mid / \mid S \mid \geq 1/\kappa(S)$. Therefore

$$\min \{ \mid X \mid / \mid S \mid : S + X \text{ singular} \} = 1/\kappa(S).$$

§

Since S is singular if and only if A is singular, we are guaranteed that minimization of $\kappa(S)$ will increase the distance between A and the set of singular matrices.

Results similar to those presented in this section can be given for triangular elements.

3 Optimization-based Smoothing Techniques

We derive two objective functions using the element condition number that are useful for optimization-based mesh improvement. We also derive an objective function based on the determinant of the Jacobian that is useful for mesh untangling. We then briefly describe the three algorithms used for optimizing the objective functions. In each case we give references to previously published work for more detailed descriptions.

3.1 Optimization Objective Functions

To build objective functions for mesh improvement based on the condition number of the tetrahedron, consider a node in the interior of a valid tetrahedral mesh with M attached tetrahedra. Let A_m be the Jacobian matrix corresponding to the mth element and $S_m = A_m W^{-1}$. Let $\kappa_m = \kappa(S_m)$,

$m = 0, 1, ..., M - 1$ be the weighted condition number of the mth attached tetrahedron normalized so that an equilateral tetrahedra has a κ value of one, and $K = (\kappa_0, \kappa_1, ..., \kappa_{M-1})$. The vector p-norm of K can be used to construct a local objective function to minimize the condition number

$$\mid K \mid_p = [\sum_{m=0}^{M-1} \kappa_m^p]^{1/p}.$$

The choice $p = 2$ gives the ℓ_2 norm of K

$$\mid K \mid_2 = [\sum_{m=0}^{M-1} \kappa_m^2]^{1/2}, \tag{1}$$

which can be used to minimize the average condition number, while $p \to \infty$ gives the ℓ_∞ norm

$$\mid K \mid_\infty = \max_m \{\kappa_m, \} \tag{2}$$

which can be used to minimize the maximum condition number. For the results presented in Section 4, we reformulate the objective function as the equivalent maximization problem as follows:

$$K_{min} = \min_m \{-\kappa_m\}. \tag{3}$$

Because the condition number goes to infinity as α goes to zero, one must begin optimization with a valid mesh. To achieve this, the mesh is preprocessed with an untangling objective function. Let α_m, $m = 0, 1, ..., M - 1$ be the Jacobian determinant of the mth attached tetrahedron and $\mathcal{A} = (-\alpha_0, -\alpha_1, ..., -\alpha_{M-1})$. Because α_m corresponds to the volume of tetrahedron m, we can use the following to create an objective function suitable for mesh untangling:

$$\mathcal{A}_{max} = \max_m \{-\alpha_m\}.$$

As with the ℓ_{inf} objective function, we can reformulate this into an objective function for the equivalent maximization problem using α_m rather than $-\alpha_m$:

$$\mathcal{A}_{min} = \min_m \{\alpha_m\}. \tag{4}$$

This is the form of the objective function used for the results presented in Section 4.

We note that some optimization techniques require the gradient of the condition number $\kappa(S)$ with respect to the free vertex position $\mathbf{x}$. Let $S = AW^{-1}$, $\sigma = det(S)$. One can apply the chain rule and the formulas given in [14] to compactly write the gradient:

$$\nabla \kappa = -\frac{\partial \kappa}{\partial S} W^{-T} u$$

with $u^T = [1, 1, 1]$. An explicit calculation shows that

$$\begin{aligned}
\frac{\partial \kappa}{\partial S} &= \frac{\mid S \mid^2 S}{\sigma^2 \kappa(S)} [\mid S \mid^2 I - S^T S] - \kappa(S) S^{-T} \\
&+ \mid S^{-1} \mid^2 \frac{S}{\kappa(S)}.
\end{aligned}$$

3.2 Optimization Procedures

We now formulate the optimization problem associated with each of the objective functions given above. In each case, the characteristics of the objective function demand different solution techniques, and we briefly describe the methods used.

Optimization of the ℓ_2 objective function. The formulation of the optimization problem for the ℓ_2 objective function given in (1) is

$$\min [\sum_{m=0}^{M-1} \kappa_m(\mathbf{x})^2]^{1/2}. \tag{5}$$

This objective function is smooth with continuous derivatives, and the problem can be solved with various techniques for unconstrained optimization.

For gradient-based optimization of the ℓ_2 objective function, one can use the expression given in [14]. However, attempts to apply a gradient-based approach to the condition number objective function were unsuccessful. The difficulty may have been due to the fact that the objective function is not continuous over all of R^3, that is, singularities in the objective function occur when the elements have zero-volume. A more sophisticated approach may overcome the problem.

For the time being, we use a robust minimization algorithm that requires only objective function values. M search directions are computed from the sum of $e_{n+1,n}$ for each of the attached tetrahedra. The objective function is then evaluated at various distances along the scaled search directions, and the node is moved to the position that provides the greatest decrease in the value of the objective function. If no decrease is found, the node is not moved. More precisely, let x be the current node position. Set toler-

ance $\epsilon = 1^{-4}$ and stopping criteria $\tau = 1^{-5}$, $\sigma_0 = 1$, $\sigma_m = 1^{-3}$, and $flag = true$.

> *while (flag)*
>   *flag = false*
>   *compute $f(x)$*
>   *$\sigma = \sigma_0$*
>   *while ($\sigma > \sigma_m$)*
>   *$\sigma = \sigma/8$*
>   *$x_{new} = x$, $f_{new} = 1^{20}$*
>   *loop over M attached elements*
>   *$\tilde{x} = (1 - \sigma)\, x + (x_{n+1} + x_{n+2} + x_{n+3})/2$*
>   *compute $f(\tilde{x})$*
>   *if ($f(\tilde{x}) < f_{new}$), $f_{new} = f(\tilde{x})$, $x_{new} = \tilde{x}$*
>   *end loop over elements*
>   *if ($f - f_{new} > \epsilon\,|\,f\,|$)*
>   *$d = |\, x - x_{new}\,|$*
>   *$x = x_{new}$*
>   *$\sigma = 0$*
>   *if ($d > \tau$), flag = true*
>   *end while*
> *end while*

Optimization of the ℓ_{inf} objective function. The optimization problem for the ℓ_{inf} objective function given in (3) is formulated as

$$\max_{} \min_{0 \le m \le M-1} \left\{ -\kappa_m(\mathbf{x}) \right\},$$

where each κ_m is a nonlinear, smooth, and continuously differentiable function of the free vertex position. Let the maximum value of the functions evaluated at $\mathbf{x}$ be called the *active value*, and the set of functions that obtain that value, the *active set*, be denoted by $\mathcal{S}(\mathbf{x})$. Because multiple elements can obtain the maximum value, the composite objective function has discontinuous partial derivatives where the active set changes from one set of functions to another set.

We solve this nonsmooth optimization problem using an analogue of the steepest descent method for smooth functions. The search direction, $\mathbf{s}$, at each step is the steepest descent direction derived from all possible convex linear combinations of the gradients in $\mathcal{S}(\mathbf{x})$. The line search subproblem along $\mathbf{s}$ is solved by predicting the points at which the active set $\mathcal{S}$ will change. These points are found by computing the intersection of the projection of a current active function in the search direction with the linear approximation of each $-\kappa_m(\mathbf{x})$ given by the first-order Taylor series approximation. The distance to the nearest intersection point from the current

location gives the initial step length, β. The initial step is accepted if the actual improvement achieved by moving v exceeds 90 percent of the estimated improvement or the subsequent step results in a smaller function improvement. Otherwise, β is halved recursively until a step is accepted, or β falls below some minimum step length tolerance. More detail on this optimization algorithm can be found in [11, 7].

Optimization of the mesh untangling objective function. The formulation of the optimization problem for the mesh untangling objective function given in (4) is

$$\max_{} \min_{0 \le m \le M-1} \left\{ \alpha_m(\mathbf{x}) \right\}, \qquad (6)$$

where α_m is a linear function of the free vertex position, $\mathbf{x}$. Thus, the solution of the optimization problem can be formulated as a linear programming problem, the details of which are given in [10].

The problem is well posed if (1) the vertices of the subproblem do not all lie in a lower-dimensional subspace than the original problem and (2) none of the vertices are co-located at the same point in space. If the problem is well posed, it is solved by using the computationally inexpensive and robust simplex method. For well posed problems, we proved that the level sets of the objective functions are convex in both two and three dimensions and, hence, the local subproblem is guaranteed to converge.

We note that optimizing α_m results in poor-quality meshes because the technique has no motivation to create good-quality elements. In fact, this technique can distort small equilateral elements in an effort to increase their volume. In practice, meshes untangled by this procedure often contain elements with angles as small as 10^{-3} degrees, and this technique must be followed by one or more of the mesh improvement techniques discussed previously.

4 Numerical Experiments

We now demonstrate the effectiveness of each of the optimization techniques in improving tetrahedral meshes compared with a baseline Laplacian smoother. We use four tetrahedral meshes generated by the CUBIT package [5] for duct, gear, hook, and foam geometries. These meshes are shown in Figure 3. In Table 1, we give the number of elements in each mesh, N, and the initial mesh quality as measured
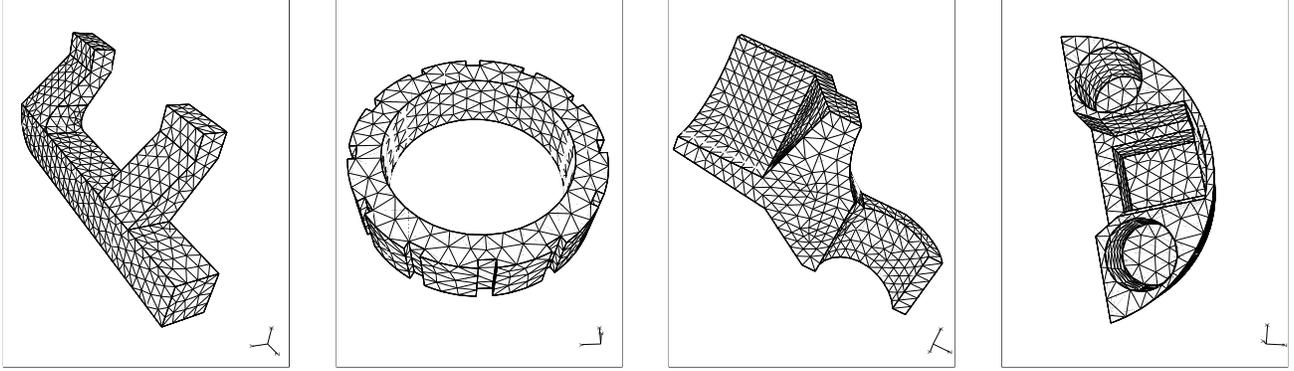
Figure 3: The four tetrahedral mesh test cases for duct, gear, hook and foam geometries

by the following metrics:

1. The number of slivers in the mesh, N_S, namely those with a normalized condition number greater than 3.0.

2. The average normalized condition number for all of the elements in the mesh, κ_{avg}.

3. The maximum normalized condition number of any element in the mesh, κ_{max}.

4. The average and maximum tetrahedral aspect ratio given by the sum of the edge lengths squared divided by the volume of the element, $A_{\gamma_{avg}}$ and $A_{\gamma_{max}}$, respectively [17]. This metric is reported to provide a comparison between the new condition number metric and a metric that is familiar to most readers.

Both the condition number and aspect ratio quality measures are normalized so that a value of one corresponds to an equilateral tetrahedron, and increasingly larger values correspond to increasingly distorted tetrahedra. The overall quality of each initial mesh as measured by κ_{avg} and $A_{\gamma_{avg}}$ is quite good, but each mesh contains a number of sliver elements.

Mesh improvement results are obtained by using the CUBIT and Opt-MS [8] software packages developed at Sandia National Laboratories and Argonne National Laboratory, respectively. An interface between these two packages has been developed, and we also report the results of a combined optimization approach that uses the two software packages in concert. We will measure the success of our smoothing techniques by their ability to eliminate sliver elements

and to reduce both the average and the maximum quality metric values.

4.1 Mesh Improvement by Condition Number Optimization

We now present results for the ℓ_2 and ℓ_{inf} smoothers using the condition number objective functions described in Section 3. We attempt to improve each initial mesh described in Table 1 with six different smoothing techniques:

1. Laplacian smoothing;

2. "smart" Laplacian smoothing, which accepts a Laplacian step only if the local submesh is improved as measured by the maximum condition number;

3. ℓ_2 smoothing as described in Section 3;

4. ℓ_{inf} smoothing as described in Section 3;

5. restricted ℓ_{inf} smoothing that is applied only if $\kappa_{max} > 3.0$ in the local submesh; and

6. a combined optimization-based approach that uses ℓ_2 smoothing on each local submesh followed by the restricted ℓ_{inf} approach.

In each case, we iterate over the interior nodes in the mesh until the change in all node point positions is smaller than some tolerance.

In Table 2 we report the results of each technique in terms of the number of slivers remaining in the

Table 1: Initial quality of the four test cases

Geom.	N	N_S	κ_{avg}	κ_{max}	$A_{\gamma_{avg}}$	$A_{\gamma_{max}}$
Duct	4267	39	1.305	3.790	1.441	5.191
Gear	3116	25	1.423	3.448	1.622	4.782
Hook	4675	30	1.360	5.176	1.533	6.151
Foam	4847	47	1.392	4.362	1.579	8.197

mesh after smoothing, the values of the quality metrics, $q_i = \kappa_{avg}$, κ_{max}, $A_{\gamma_{avg}}$, $A_{\gamma_{max}}$, as well as the percentage change from the initial value as computed by the formula

$$\mathcal{P}_i = \frac{q_{i\,final} - q_{i\,initial}}{q_{i\,initial}} \times 100.$$

Because of the way the metrics are normalized, a negative $\mathcal{P}_i$ value indicates an improvement in mesh quality whereas a positive $\mathcal{P}_i$ value indicates a worsening of mesh quality. We also report the number of nodes moved during the mesh smoothing process, C_S, which corresponds to the number of calls made to each smoother. For the combined approach, C_S is reported as the number of calls to the ℓ_2 smoother, C_1, plus the number of calls to the $\ell_{\inf}$ smoother, C_2, and is denoted (C_1, C_2).

In three of the four cases, Laplacian smoothing results in a mesh containing inverted elements. The CUBIT software defines the condition number of inverted elements to be 10^6, which skews the κ_{avg} and κ_{max} values for those meshes; we do not report those results. In all four cases, Laplacian smoothing worsens mesh quality by every measure reported: the number of slivers is approximately doubled, $A_{\gamma_{avg}}$ increases by more than two percent, and $A_{\gamma_{max}}$ is significantly worsened in all four cases. By design, the "smart" Laplacian smoother improves the mesh in each case, but the improvement in the average element quality is less than .5 percent in all cases, and the improvement in the maximum quality values is zero in two of the four cases.

In contrast, the optimization-based smoothing approaches preserve mesh validity in all four test cases, and each approach significantly improves the mesh by some measure of mesh quality. Both the ℓ_2 and ℓ_{inf} smoothers are able to eliminate a majority of the slivers. The ℓ_{inf} smoother typically does better than ℓ_2 with respect to this metric, and in two of the four cases eliminates all of the slivers from the mesh. As expected, the ℓ_2 smoother improves the average element quality in all four cases by as much 3.2 percent.

Although it is not designed to improve κ_{max}, this can happen serendipitously as is evidenced in three of the four cases. In the gear geometry, however, κ_{max} worsens by about 6 percent. The results for the ℓ_{inf} smoother are the inverse of the ℓ_2 results. The average element quality is worsened in each case by as much as 5.7 percent in the duct geometry, but the κ_{max} and $A_{\gamma_{max}}$ values are always significantly improved. The restricted ℓ_{inf} smoother achieves nearly the same improvement in κ_{max} and $A_{\gamma_{max}}$ as the ℓ_{inf} smoother without the corresponding decrease in average element quality. The combined optimization approach achieves the best overall improvement in each of the four cases; all quality metrics are significantly improved in all test cases, and its use is recommended.

In each case the number of calls to the ℓ_2 smoother is roughly equal to the number of vertices in the mesh; that is, each local submesh is visited approximately only once. In contrast the ℓ_{inf} smoother is called more times, indicating more grid point movement. This is supported by the fact that the average element quality changes approximately twice as much when the ℓ_{inf} smoother is called significantly more times than the ℓ_2 smoother. The restricted ℓ_{inf} smoother is called approximately once for each sliver in the mesh when used alone, and far fewer times when used in conjunction with the ℓ_2 smoother. Currently the ℓ_{inf} and ℓ_2 smoothers are about ten and one hundred times more expensive than smart Laplacian, respectively, and work to reduce computational cost is under way.

4.2 Mesh Untangling and Improvement

To demonstrate the effectiveness of optimization-based untangling, we used a randomized smoothing scheme on the original meshes given in Table 1 to create "tangled" meshes with valid connectivity but several hundred inverted elements. In Table 3, we give the number of inverted elements, N_I, the number

Table 2: Mesh quality improvement results for the optimization-based smoothing techniques

Technique	N_S ($\mathcal{P}$)	κ_{avg} ($\mathcal{P}$)	κ_{max} ($\mathcal{P}$)	$A_{\gamma_{avg}}$ ($\mathcal{P}$)	$A_{\gamma_{max}}$ ($\mathcal{P}$)	C_S
Duct Geometry						
Laplacian	78 (+100)	–	–	1.452 (+.76)	24.25 (+367)	1303
Smart Lap.	31 (-20.5)	1.300 (-.38)	3.691 (-2.6)	1.433 (-.56)	4.964 (4.3)	732
ℓ_2 Opt.	15 (-62)	1.275 (-2.2)	3.690 (-2.6)	1.400 (-2.8)	4.578 (-11.8)	2773
ℓ_{inf} Opt.	4 (-90)	1.379 (+5.7)	3.045 (-19.7)	1.571 (+9.0)	3.979 (-23.3)	5498
Restricted ℓ_{inf}	4 (-90)	1.313 (+.61)	3.045 (-19.7)	1.493 (+3.6)	3.979 (-23.3)	32
Combined	4 (-90)	1.280 (-2.2)	3.045 (-19.7)	1.409 (-2.2)	3.980 (-23.3)	(2773,13)
Gear Geometry						
Laplacian	63 (+152)	–	–	1.661 (+2.4)	84.80 (+1673)	1051
Smart Lap.	11 (-56)	1.414 (-.63)	3.309 (-4.0)	1.610 (-.74)	4.782 (0)	492
ℓ_2 Opt.	3 (-88)	1.378 (-3.2)	3.657 (+6.1)	1.560 (-3.8)	5.201 (+8.8)	2141
ℓ_{inf} Opt.	0 (-100)	1.455 (+2.2)	2.996 (-13.1)	1.682 (+3.6)	3.703 (-22.5)	2213
Restricted ℓ_{inf}	0 (-100)	1.425 (+.14)	2.996 (-13.1)	1.627 (+.31)	4.744 (-13.1)	24
Combined	0 (-100)	1.380 (-3.0)	2.996 (-13.1)	1.562 (-3.6)	3.953 (-17.3)	(2141,3)
Hook Geometry						
Laplacian	64 (+113)	1.393 (+2.4)	74.28 (+1335)	1.569 (+2.3)	88.19 (+1334)	1443
Smart Lap.	27 (-10)	1.356 (-.25)	5.176 (0)	1.529 (-.26)	6.151 (0)	798
ℓ_2 Opt.	7 (-77)	1.331 (-2.1)	3.747 (-27.6)	1.495 (-2.4)	4.437 (-27.9)	2933
ℓ_{inf} Opt.	0 (-100)	1.429 (+5.1)	2.973 (-48.0)	1.659 (+8.2)	4.331 (-29.6)	5970
Restricted ℓ_{inf}	0 (-100)	1.367 (+.51)	2.990 (-42.2)	1.549 (+1.0)	4.331 (-29.6)	34
Combined	0 (-100)	1.332 (-2.1)	2.973 (-42.6)	1.497 (-2.3)	4.331 (-29.6)	(2933,5)
Foam Geometry						
Laplacian	82 (+74)	–	–	1.622 (+2.7)	83.17 (+914)	916
Smart Lap.	42 (-11)	1.390 (-.14)	4.362 (0)	1.575 (-.25)	8.197 (0)	555
ℓ_2 Opt.	21 (-55)	1.372 (-1.4)	4.310 (-1.2)	1.552 (-1.7)	6.760 (-17.5)	2637
ℓ_{inf} Opt.	25 (-47)	1.447 (+4.0)	4.310 (-1.2)	1.672 (+5.8)	6.596 (-19.5)	3376
Restricted ℓ_{inf}	25 (-53)	1.398 (+.43)	4.310 (-1.2)	1.590 (+.70)	6.596 (-19.5)	33
Combined	24 (-49)	1.375 (-1.2)	4.310 (-1.2)	1.556 (-1.4)	6.596 (-19.5)	(2637,11)

of sliver elements, N_S, as well as the quality metrics κ_{avg}, κ_{max}, $A_{\gamma_{avg}}$, and $A_{\gamma_{max}}$ for each of the four tangled meshes. The results of the untangling procedure described in Section 3 are reported for each geometry in the rows labeled "Untangle". In each case the optimization-based procedure successfully eliminates all of the inverted elements from the mesh, but, as expected, the resulting mesh quality is quite poor. We therefore follow the untangling procedure with the combined optimization approach described in the previous section. In each case, even though we are starting from a significantly worse-quality mesh, we obtain the nearly same final mesh quality as reported in Table 2.

5   Conclusions

Our results indicate that Laplacian smoothing can be detrimental to the quality of simplicial meshes on complex geometries, and we do not recommend its use. In contrast, the optimization approaches, particularly the combined ℓ_2 and ℓ_{inf} smoothing technique, significantly improved the quality of each of the test cases. We showed that the behavior of the more commonly accepted aspect ratio shape measure was mirrored by the behavior of the condition number shape measure, and that the condition number shape measure is theoretically optimal.

Strategically combining different local mesh smoothing strategies is not a new idea; a number of researchers have combined Laplacian smoothing with

Table 3: Mesh quality improvement results for the optimization-based smoothing techniques

Technique	N_I	N_S	κ_{avg}	κ_{max}	$A_{\gamma\,avg}$	$A_{\gamma\,max}$	C_U	C_S
Duct Geometry								
Tangle	402	1049	–	–	6.321	72.09	–	–
Untangle	0	75	1.318	11.06	1.393	24.72	2068	–
Combined	0	4	1.281	3.045	1.409	3.980	–	(2954,14)
Gear Geometry								
Tangle	297	764	–	–	20.63	3.95^4	–	–
Untangle	0	56	1.477	89.24	1.688	125.9	1785	–
Combined	0	0	1.380	2.996	1.562	3.809	–	(2305,3)
Hook Geometry								
Tangle	515	1252	–	–	7.559	2.43^3	–	–
Untangle	0	58	1.381	38.86	1.558	45.91	2557	–
Combined	0	0	1.332	2.973	1.497	4.331	–	(3160,5)
Foam Geometry								
Tangle	299	828	–	–	4.419	1.07^3	–	–
Untangle	0	82	1.419	49.91	1.609	60.17	1580	–
Combined	0	24	1.375	4.310	1.555	6.709	–	(2760,11)

their optimization-based approaches to achieve good quality meshes at a low computational cost [19, 7]. However, this is the first instance we are aware of in which two optimization strategies have been combined to improve both the average element quality and the extremal element quality. Although our results showed that these improvements can be achieved for a small incremental cost to the ℓ_2 strategy, further work is needed to reduce the overall cost of the approach. Techniques that combine Laplacian smoothing with the combined technique presented here are under consideration.

Finally, we note that the algorithms presented in this paper for smoothing and untangling are local techniques; a globally optimal solution is not guaranteed although empirical evidence suggests that the techniques work well in practice. We suspect that a global convergence proof for the simplicial mesh untangling algorithm is possible. That is, given assumptions of topological validity in the mesh and boundary correctness, the linear programming approach will successfully untangle the mesh. Future work will include a formal proof to determine the exact geometrical and topological assumptions under which the global convergence is possible.

Acknowledgments

References

[1] R. E. Bank and R. K. Smith. Mesh smoothing using a posteriori error estimates. *SIAM Journal on Numerical Analysis*, 34(3):979–997, June 1997.

[2] Randy Bank. *PLTMG: A Software Package for Solving Ellipitc Parital Differential Equations, Users' Guide 7.0*, volume 15 of *Frontiers in Applied Mathematics*. SIAM, Philadelphia, 1994.

[3] J. Demmel. *Applied Numerical Linear Algebra.* SIAM, Philadelphia, Pennsylvania, 1997.

[4] J. Dompierre, P. Labbe, F. Guibault, and R. Camerero. Proposal of benchmarks for 3d unstructured tetrahedral mesh optimization. In *Proceedings of the 7th International Meshing RoundTable'98*, pages 459–478, 1998.

[5] T. D. Blacker et. al. CUBIT mesh generation environment. Technical Report SAND94-1100, Sandia National Laboratories, Albuquerque, New Mexico, May 1994.

[6] David A. Field. Laplacian smoothing and Delaunay triangulations. *Communications and Applied Numerical Methods*, 4:709–712, 1988.

[7] Lori Freitag. On combining Laplacian and optimization-based smoothing techniques. In *Trends in Unstructured Mesh Generation*, volume AMD-Vol. 220, pages 37–44. ASME Applied Mechanics Division, 1997.

[8] Lori Freitag. Users manual for Opt-MS: Local methods for simplicial mesh smoothing and untangling. Technical Report ANL/MCS-TM-239, Mathematics and Computer Science Division, Argonne National Laboratory, Argonne, Ill., 1999.

[9] Lori Freitag and Carl Ollivier-Gooch. A comparison of tetrahedral mesh improvement techniques. In *Proceedings of the Fifth International Meshing Roundtable*, pages 87–100. Sandia National Laboratories, 1996.

[10] Lori Freitag and Paul Plassmann. Local optimization-based simplicial mesh untangling and improvement. Preprint ANL/MCS-P749-0399, Mathematics and Computer Science Division, Argonne National Laboratory, Argonne, Ill., August, 1999.

[11] Lori A. Freitag, Mark T. Jones, and Paul E. Plassmann. An efficient parallel algorithm for mesh smoothing. In *Proceedings of the Fourth International Meshing Roundtable*, pages 47–58. Sandia National Laboratories, 1995.

[12] P. L. George and H. Borouchaki. *Delaunay Triangulation and Meshing.* Hermes, Paris, 1998.

[13] Patrick Knupp. Achieving finite element mesh quality via optimization of the Jacobian matrix norm and associated quantities, Part I - A framework for surface mesh optimization. Technical Report SAND 99-0110J, Sandia National Laboratories, 1999.

[14] Patrick Knupp. Achieving finite element mesh quality via optimization of the Jacobian matrix norm and associated quantities, Part II - A framework for volume mesh optimization. Technical Report SAND 99-0709J, Sandia National Laboratories, 1999.

[15] A. Liu and B. Joe. Relationship between tetrahedron quality meausres. *BIT*, 34:268–287, 1994.

[16] S. H. Lo. A new mesh generation scheme for arbitrary planar domains. *International Journal for Numerical Methods in Engineering*, 21:1403–1426, 1985.

[17] V. N. Parthasarathy, C. M. Graichen, and A. F. Hathaway. A comparison of tetrahedron quality measures. *Finite Element Analysis and Design*, 15:255–261, 1993.

[18] Matthew L. Staten Scott A. Canann, Joseph R. Tristano. An approach to combined Laplacian and optimization-based smoothing for triangular, quadrilateral, and quad-dominant meshes. In *Proceedings of the 7th International Meshing Roundtable*, pages 479–494. Sandia National Laboratories, 1998.

[19] Mark Shephard and Marcel Georges. Automatic three-dimensional mesh generation by the finite octree technique. *International Journal for Numerical Methods in Engineering*, 32:709–749, 1991.